IOP PUBLISHING JOURNAL OF PHYSICS D: APPLIED PHYSICS

J. Phys. D: Appl. Phys. **43** (2010) 505305 (5pp) doi:10.1088/0022-3727/43/50/505305

Transport behaviours and nanoscopic resistance profiles of electrically stressed Pt/TiO_2/Ti planar junctions

Haeri Kim[1], **Dong-Wook Kim**[1,2] **and Soo-Hyon Phark**[3]

[1] Department of Physics, Ewha Womans University, Seoul 120-750, Korea
[2] Department of Chemistry and Nano Science, Ewha Womans University, Seoul 120-750, Korea
[3] Max-Planck-Institut für Mikrostrukturphysik, Weinberg 2, D-06120 Halle, Germany

E-mail: dwkim@ewha.ac.kr

Received 9 June 2010, in final form 24 October 2010
Published 2 December 2010
Online at stacks.iop.org/JPhysD/43/505305

Abstract
Using Pt/TiO_2/Ti planar junctions fabricated with micrometre-sized gaps between electrodes, we found that the application of a bias voltage between the electrodes significantly decreased the resistance of the junction. The nanoscopic resistance profile revealed that the electrical stress modified the bulk as well as the contact resistance. Electrostatic force microscopy was used to investigate the charge distribution and its time evolution in local areas scanned by positively biased Pt-coated tips. Comparative investigations of the transport and scanning probe microscopy results suggest that the electrical stress induced a redistribution of ions, which then modified the junctions' transport characteristics.

(Some figures in this article are in colour only in the electronic version)

1. Introduction

As a result of their importance in non-volatile memory applications, resistive switching (RS) phenomena in metal/oxide/metal (MOM) structures have attracted a great deal of research interest [1–14]. Intensive investigations have suggested that coupled electron–ion dynamics play a key role in bi-stable resistance states [1–12]. The total resistance of an MOM structure is the sum of its contact and bulk resistances. It is not yet completely understood how ionic drift and diffusion affects the contact and bulk contributions to transport and RS [1–8].

In thin films, structural defects (e.g., grain boundaries) and compositional inhomogeneity can provide preferential electronic and ionic transport paths [1, 13]. As a result, otherwise identical materials have shown significantly different transport and resulting RS behaviours, depending on the microstructural properties of the samples [3–8]. Single crystals, with their negligible crystalline disorder and compositional variation, enable us to rule out such complications. The examination of single crystalline samples will be useful for discovering the inherent nature of ionic-migration-related transport [8–11].

In this study, we fabricated metal/TiO_2 single crystal/metal planar junctions with micrometre-sized gaps. Two different electrode materials were used to form Schottky and Ohmic contacts to the TiO_2, so as to separate and understand the contact and bulk contributions to the transport phenomena. To lend an additional insight into the understanding of the underlying mechanisms, scanning Kelvin probe microscopy (SKPM) and electrostatic force microscopy (EFM) were used to examine both the local electrical properties in response to an applied voltage stress and its time evolution at the TiO_2 surface.

2. Experiment

This study was conducted using 0.5 mm thick TiO_2(1 0 0) single crystals (CrysTec., GmbH., Germany) annealed for 1 h at 450 °C in a forming gas of 5% hydrogen and 95% nitrogen to induce an oxygen-deficient layer near the surface [3, 8]. An RF sputtering system was used to deposit 50 nm thick Pt and 50 nm Pt/10 nm Ti electrodes onto a TiO_2 surface. The Ti layers were capped with a Pt layer to prevent oxidation. Hereafter, the Pt/Ti electrodes will be simply called Ti electrodes. The 4 μm wide

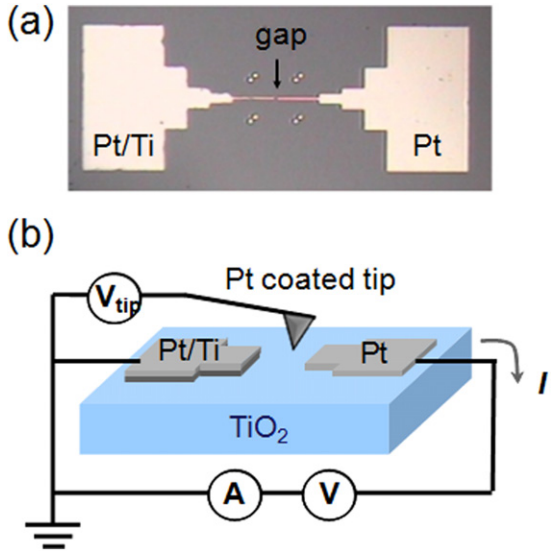

Figure 1. (*a*) Optical microscope image of a Pt/TiO_2/Ti planar junction and (*b*) a schematic diagram of experimental configuration for transport and SPM measurements.

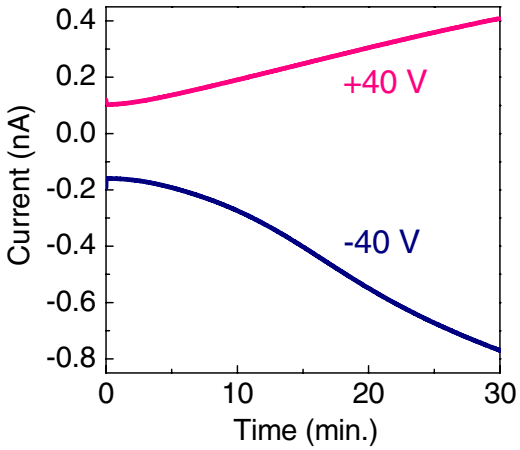

Figure 2. Current versus time curves of Pt/TiO_2/Ti planar junctions during electrical stress, i.e. application of a large voltage (±40 V) to the electrodes.

electrodes were patterned with several micrometres gap along the [0 0 1] direction of the TiO_2 single crystals by conventional photolithography and a lift-off process. An optical microscope image and a schematic diagram of the Pt/TiO_2/Ti planar junction are shown in figures 1(*a*) and (*b*). The transport characteristics were investigated using a Hewlett-Packard 4156B semiconductor parameter analyzer (SPA).

SKPM and EFM measurements were done using scanning probe microscopy (SPM) systems (Park Systems Co. and Nanofocus Co., Korea). During the SPM measurements, Pt-coated Si cantilevers were used in non-contact mode and the applied bias to the tip had both ac and dc components, $V_{tip} = V_{dc} + V_{ac} \cos \omega t$. Specific frequency component amplitude of F_e could be extracted by a lock-in amplifier (SR830, Stanford Research Systems Inc., USA). Transport and SPM measurements could be performed for an identical sample, as illustrated in figure 1(*b*).

3. Results and discussion

To impose an electrical stress, large voltages of ±40 V were applied to the Pt/TiO_2/Ti planar junctions. We defined the current direction from the Pt electrode to the Pt/Ti electrode as positive, and the opposite direction as negative. The current gradually increased during both the positive and negative stresses as shown in figure 2. The total resistance of the Pt/TiO_2/Ti junctions (R_{Total}) should be the sum of the Pt/TiO_2 contact resistance ($R_{C,Pt}$) and the TiO_2 bulk resistance (R_B). The applied voltage divides into the contact and bulk regions, and the electric field in each region is determined by the contact-to-bulk resistance ratio. Application of an electric field and resulting transport properties of Pt/TiO_2 contacts were reported by many researchers [3–6]. It has been believed that the electric-field-induced oxygen vacancy drift towards the Pt electrode and the accumulated vacancies under the negative terminal eliminated the Schottky barrier, resulting in a lowering of $R_{C,Pt}$. However, any change in R_B has not been explicitly addressed. Our asymmetric Pt/TiO_2/Ti junctions showed that R_{Total} was reduced irrespective of the programming voltage polarity. This suggests that R_B as well as $R_{C,Pt}$ decreased, since the decrease in $R_{C,Pt}$ under positive stress was hardly expected [3–6].

Figure 3 shows the time evolution of the transport characteristics for the Pt/TiO_2/Ti planar junction after 30 min of electrical stress. After a sufficient time, the I–V curves return to their initial values. This suggests that the resistance reduction is not caused by any irreversible structural or chemical changes during the electrical stress. The I–V curves after the negative stress are nearly linear in the whole voltage range, whereas those after the positive stress are nonlinear in the low voltage region ($|V| <\sim 2$ V). The negative stress can lower the Pt/TiO_2 Schottky contact resistance and allow Ohmic transport. The transport after the positive stress, however, is still limited by the Schottky contact, and exhibits small current and nonlinear behaviour. All the I–V curves in figures 3(*a*) and (*b*) do not show rectifying behaviour, since the junctions have large R_B and the voltage drop to the contact may not be large enough to turn on the Schottky diode in the measurement voltage range ($|V| < 10$ V).

Figure 4 shows the resistance profile of the junctions, before and after the electrical stress. Surface potential distributions were measured while applying +5 V between the electrodes, and resistance of a certain region could be roughly estimated by (potential drop for the chosen region)/(current). The resistance profiles clearly show that there is an abrupt potential drop at the Pt/TiO_2 contact but not at the Ti/TiO_2 contact. This means that the resistance of the former is much larger than that of the latter, as anticipated from the work function difference [3, 9]. The negative electrical stress (−40 V, 30 min.) resulted in decrease in the junction resistance, especially notable reduction in the contact resistance. This assures the barrier height lowering, as suggested earlier [3–6]. In contrast, the positive electrical stress (+40 V, 30 min.) did not affect $R_{C,Pt}$ but reduced R_B. Such a result is consistent with our explanations inferred from the I–V curves in figure 3(*a*).

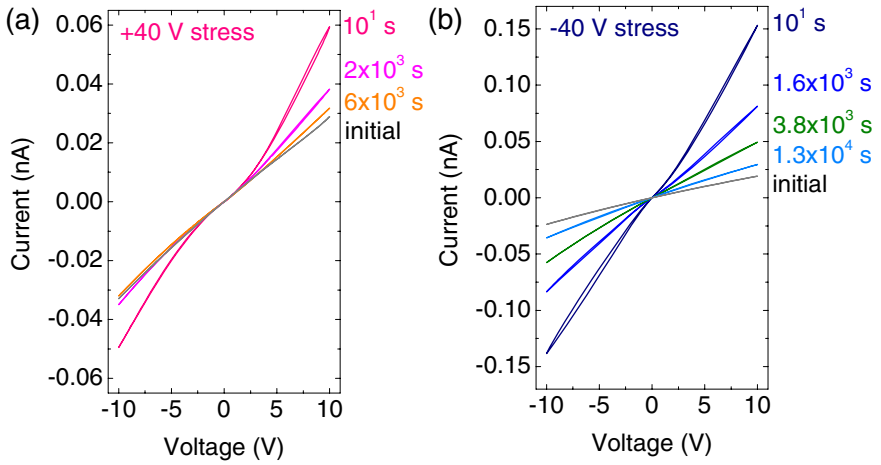

Figure 3. Time-dependent current–voltage characteristics of a Pt/TiO_2/Ti junction for (*a*) positive and (*b*) negative electrical stress. Elapsed time after the electrical stress is indicated near each curve.

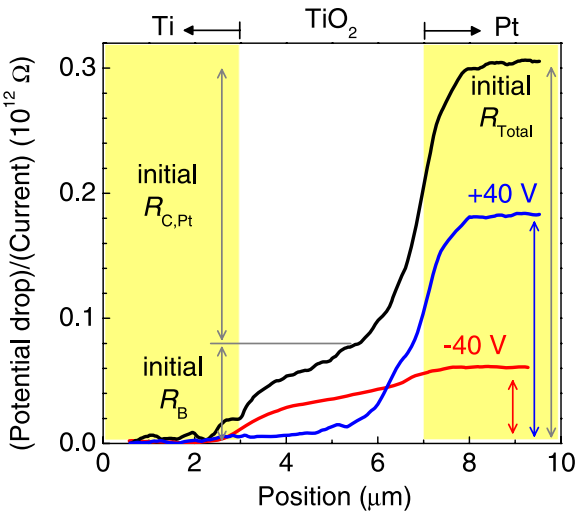

Figure 4. Resistance of the junctions as a function of position. Black, red and blue lines are from the initial, −40 V stressed and +40 V stressed states, respectively.

The electric-field-induced drift during the electrical stress can cause the $R_{C,Pt}$ change, as discussed above. The oxygen vacancy drift time was estimated in our device geometry, as τ_{drift} = (gap distance)/[(ionic mobility) × (electric field)] = 8.0×10^6 s, which is much longer than the 30 min electrical stress exposure in our experiments [6]. Such a large difference may indicate that the active region required to induce the resistance change can be much smaller than the whole device size. For example, a recent theoretical work suggested that the barrier height can be varied by atomic-scale movement of the oxygen vacancies at the Pt/TiO_2 interface [11]. In addition, some other possibilities to decrease the drift time can be suggested. As revealed in figure 4, the Pt/TiO_2 contact has notable potential drop at the interface and the electric field underneath the Pt electrode would be very large. If the field is sufficiently large, rapid increase in the drift velocity can be expected according to the exponential ionic drift behaviour [12]. Since the reduced TiO_2 sample surface can be more conducting than the bulk underneath, Joule heating may occur and enhance the ionic mobility during the electrical stress. If the vacancies form local conducting paths, they can also thermally enhance activated ionic drift [6, 10].

After removal of the electric field, the vacancies will suffer diffusion due to the concentration gradient and the junctions will return to the initial states. The diffusion constant, D_V, of oxygen vacancies in TiO_2 is known to be 6.46×10^{-18} cm^2 s^{-1} [6], and the ion diffusion time from one electrode to the other for our junction can be estimated as $\tau_{diffusion}$ = (gap distance)$^2/D_V$ = 6.1×10^9 s. This is too long, compared with the experimental retention time of several hours. If the change in $R_{C,Pt}$ is caused by the ionic drift in the atomic scale as mentioned above, the length scale for the diffusion to cause the retention should be comparable. For example, the diffusion time for a distance of 1 nm would be 1.5×10^3 s for TiO_2, which is comparable to the measured retention time (figure 3).

Figure 4 clearly showed that not only $R_{C,Pt}$ but also R_B was reduced irrespective of the bias polarity during the electrical stress. According to the estimated drift and diffusion time above, it is hard to expect that the vacancy migration scenario can explain the R_B change. This means that another factor to influence R_B should be considered. Our reduced TiO_2 samples can have higher vacancy concentration near the surface [3, 8]. Thus, the bulk TiO_2 can be regarded as parallelly connected resistors, with a larger proportion in the conducting surface region and less in the conducting bulk region. In very thin films and nanostructures, the carrier concentration can be affected by adsorption of gas molecules from the ambient. For *n*-type metal oxides including TiO_2, it is known that oxygen molecules adsorbed on the surface can capture electrons from the oxides [$O_2(g) + e^- \rightarrow O_2^-(ad)$] and induce the surface depletion region [15]. Therefore, the changes in R_B can be understood based on any change in the amount of adsorbed gas molecules and resulting effective carrier concentration at the TiO_2 surface region. In ZnO-based gas sensors, electric-field-induced gas desorption was reported [17]. Similar electro-desorption might occur in our junctions during the electrical stress. In addition, Joule heating during the electrical stress may help desorption of adsorbed ions at the surface and reduce R_B. Although the

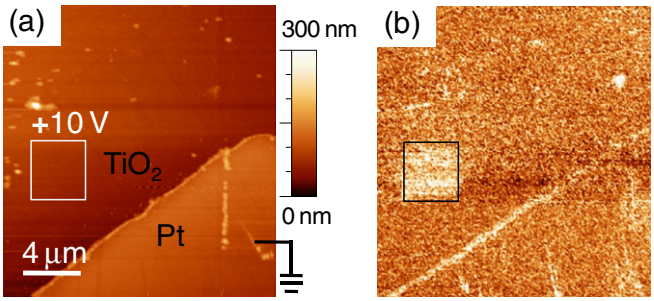

Figure 5. (*a*) Topographic image of a Pt/TiO_2/Ti junction indicating regions affected by positive-tip stress and (*b*) EFM image obtained after the tip-induced stress.

experimental data manifest the electric-field-induced alteration of R_B, complete understanding of the physical origins is lacking at the present moment.

The distribution of the ions, near the surface, can affect the time evolution of R_B due to the aforementioned reasons. EFM imaging will reveal the local charge distribution at the TiO_2 surface. As shown in figure 5(*a*), a large dc voltage ($\pm$10 V) was applied over 4 μm $\times$ 4 μm areas for 256 s using the EFM tip. Such a step would modify the surface charges, analogous to the application of a large voltage to the electrode during the electrical stress [18]. Hereafter, it will be referred to as 'tip-induced stress.' Figure 5(*b*) shows that the contrast in the area resulting from positive-tip-induced stress is clearly seen. However, no contrast was observed by the negative tip (data not shown). The electrostatic force between the tip and the sample, F_e, consists of capacitive and Coulombic terms and the amplitude of the ω component in F_e is proportional to the term,

$$\left(\frac{\partial C}{\partial z}(V_{dc} - V_{CPD}) + \frac{\sigma_b C}{2\varepsilon_0}\right),$$

which will be denoted as the 'EFM signal' [15]. C is the capacitance between the tip and the sample, z is the tip–sample separation, V_{dc} and V_{ac} are the dc and ac voltage amplitude applied to the tip and V_{CPD} is $\Delta W/e$ (ΔW: the tip–sample work function difference). The work function of semiconductor can be given by $W_{Sample} = (E_C - E_F) - eV_S + \chi - \Delta\phi$, where eV_S is the surface band bending and $\Delta\phi$ is the surface dipole energy [15]. If the negatively charged oxygen ions can be removed from TiO_2 by the positive tip, then the doping concentration (i.e. $E_C - E_F$) will be altered [1, 8, 12]. Some ions adsorbed on the TiO_2 surface also can be taken away during the tip-induced stress, resulting in the change in eV_S and/or $\Delta\phi$. Such desorption should vary R_B due to the surface depletion [16, 17]. Obviously, the surface ionic distribution, directly related to R_B, should affect the EFM signal.

The negative-tip stress can inject O_2^- into the TiO_2 surface, resulting in the annihilation of oxygen vacancies. This process corresponds to 'local anodic oxidation', which is sometimes intentionally used to form nanoscale oxide patterns on metal substrates [19]. As our samples are nearly stoichiometric TiO_2 single crystals, few sites exist to accept the injected O_2^-, and charge injection rarely happens. Therefore, the negative-tip stress can result in only a negligible change in the EFM

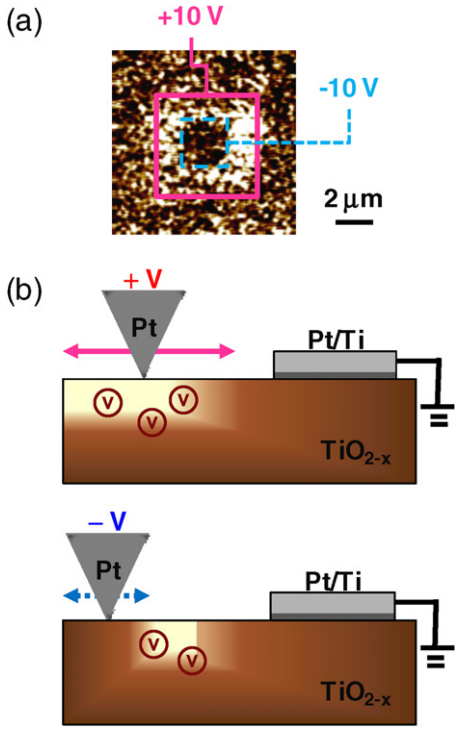

Figure 6. (*a*) EFM image of a Pt/TiO_2/Ti junction after positive- and negative-tip stress and (*b*) schematic of the tip-induced-stress processes on the TiO_2 surface.

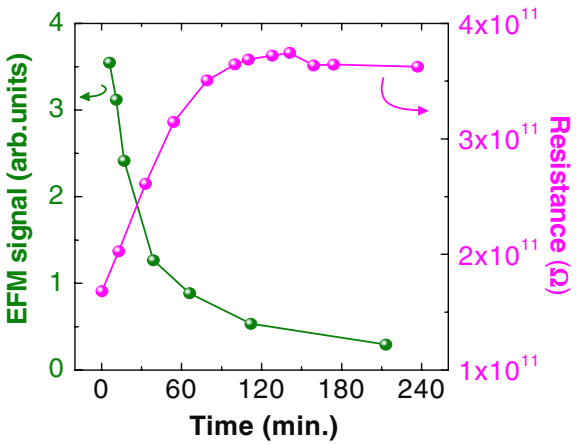

Figure 7. Time dependence of the EFM signal and R_{Total} change caused by application of +10 V to the EFM tip and −40 V to the electrodes, respectively.

contrast. To confirm our conjecture, a positive-tip stress was applied on a defined area of the TiO_2 surface and immediately performed a negative-tip stress on the central region of the positively stressed area. Subsequent EFM imaging showed that the EFM signal in the inner area was suppressed similarly to that of the non-stressed area; see figure 6(*a*). The negative tip scanning may supply oxygen ions from the ambient atmosphere and compensate the positive charge in the region stressed by the positively biased tip. This result supports our suggestion regarding the polarity dependence of the tip-induced stress, which is schematically illustrated in figure 6(*b*).

Figure 7 shows the EFM signal and the junction resistance, R_{Total}, obtained at the region by applying +10 V to the EFM

tip and −40 V to the electrodes as a function of time. Both the EFM signal and R_{Total} gradually varied and returned to their initial values after several hours. The modification of the ionic distribution and the subsequent recovery processes in our junctions can vary R_{Total}. Comparable retention time for the EFM signal and the R_{Total} confirms the relevance of the EFM signal and R_{B}, as suggested.

Jameson *et al* reported that the recovery for the resistance of their Pt/TiO_2/Pt planar junctions took several hours after the electrical stress [8]. The recovery behaviour is comparable to our result, which suggests that a similar mechanism may be involved in their experiments. Recently Oka *et al* reported that the retention time of NiO nanowire/metal junctions, exhibiting bipolar RS, strongly depended on the ambient gas [14]. The LRS resistance increased in the reduced ambient (e.g., vacuum) but decreased in the oxidizing atmosphere (e.g., ozone). Based on such results, they argued that the reaction between the p-type NiO nanowires and ambient oxygen played a crucial role in the RS behaviours. Like our Pt/TiO_2/Ti structures, the nanowire junctions are surrounded by the ambient gas and a larger portion of the junction resistance should be determined by the nanowire bulk resistance. All these suggest that the interaction of the sample with the ambient can influence the carrier distribution and transport in the metal/oxide junctions. In many of the studies, the ambient dependence has not been emphasized [1, 14]. Firstly, the contact or bulk resistance dominates in the resistance of most device structures [1, 9]. Secondly, the active device area exposed to the ambient is very limited. In integrated devices, the active RS layers may have tiny volume and can be surrounded by intermetallic dielectric layers. In such a case, the interaction (redox) between the active layers and the dielectrics would be very important for reliable device operations. The planar junctions and their SPM studies may give us valuable insights for further understanding of the RS mechanism and improvement of the RS devices.

4. Summary

We investigated the transport properties and local electrical properties of electrically stressed Pt/TiO_2/Ti planar junctions. The application of an electrical field could lower the total junction resistance and modify the charge distribution. The polarity dependence of the stress field and the time evolution of the junctions' resistance clearly revealed that the ionic distribution significantly affected the transport properties of the junctions.

Acknowledgments

This work was supported by the Quantum Metamaterials Research Center (2009-0063324) through the National Research Foundation of Korea Grant and the National Program for 0.1 Terabit NVM Devices Grant funded by the Korea government.

References

[1] Waser R, Dittmann R, Staikov G and Szot K 2009 *Adv. Mater.* **21** 2632
[2] Shima H, Takano F, Muramatsu H, Akinaga H, Tamai Y, Inoue I H and Takagi H 2008 *Appl. Phys. Lett.* **93** 113504
[3] Yang J J, Picket M D, Li X, Ohlberg D A, Stewart D R and Williams R S 2008 *Nature Nanotechnol.* **3** 429
[4] Strachan J P, Yang J J, Münstermann R, Scholl A, Medeiros-Ribeiro G, Stewart D R and Williams R S 2009 *Nanotechnology* **20** 485701
[5] Shima H, Zhong Z and Akinaga H 2009 *Appl. Phys. Lett.* **94** 082905
[6] Jeong D S, Schroeder H, Breuer U and Waser R 2008 *J. Appl. Phys.* **104** 123716
[7] Kwon D-H *et al* 2010 *Nature Nanotechnol.* **5** 148
[8] Jameson J R, Fujuzumi Y, Wang Z, Griffin P, Tsunoda K, Meijer G I and Nishi Y 2007 *Appl. Phys. Lett.* **91** 112101
[9] Park C, Seo Y, Jung J and Kim D-W 2008 *J. Appl. Phys.* **103** 054106
[10] Andreasson B P, Janousch M, Staub U, Meijer G I, Ramar A, Krbanjevic J and Schaeublin R 2009 *J. Phys. Conf. Ser.* **190** 012074
[11] Tamura T, Ishibashi S, Terakura K and Weng H 2009 *Phys. Rev.* B **80** 195302
[12] Strukov D B and Williams R S 2009 *Appl. Phys.* A **94** 515
[13] Park C, Jeon S H, Chae S C, Han S, Park B H, Seo S and Kim D-W 2008 *Appl. Phys. Lett.* **93** 042102
[14] Oka K, Yanagida T, Nagashima K, Kawai T, Kim J and Park B H 2010 *J. Am. Chem. Soc.* **132** 6634
[15] Kronik L and Shapira Y 1999 *Surf. Sci. Rep.* **37** 1
[16] Rothschild A, Levakov A, Shapira Y, Ashkenasy and Komem Y 2003 *Surf. Sci.* **532–535** 456
[17] Fan Z and Lu J G 2005 *Appl. Phys. Lett.* **86** 123510
[18] Xie Y, Bell C, Yajima T, Hikita Y and Hwang H Y 2010 *Nano Lett.* **10** 2588
[19] Kim T Y, Ricci D, Zitti E Di and Cincotti S 2007 *Surf. Sci.* **601** 4910